Statistical physics of fracture: scientific discovery through high-performance computing

Phani Kumar V. V. Nukala[1]**, Srđan Šimunović**[1]**, and Richard T. Mills**[1,]

[1] Computer Science and Mathematics Division, Oak Ridge National Laboratory, Oak Ridge, Tennessee 37831, USA

E-mail: `nukalapk@ornl.gov`

Abstract. The paper presents the state-of-the-art algorithmic developments for simulating the fracture of disordered quasi-brittle materials using discrete lattice systems. Large scale simulations are often required to obtain accurate scaling laws; however, due to computational complexity, the simulations using the traditional algorithms were limited to small system sizes. We have developed two algorithms: a multiple sparse Cholesky downdating scheme for simulating 2D random fuse model systems, and a block-circulant preconditioner for simulating 3D random fuse model systems. Using these algorithms, we were able to simulate fracture of *largest ever* lattice system sizes ($L = 1024$ in 2D, and $L = 64$ in 3D) with extensive statistical sampling. Our recent simulations on 1024 processors of Cray-XT3 and IBM Blue-Gene/L have further enabled us to explore fracture of 3D lattice systems of size $L = 200$, which is a significant computational achievement. These largest ever numerical simulations have enhanced our understanding of physics of fracture; in particular, we analyze damage localization and its deviation from percolation behavior, scaling laws for damage density, universality of fracture strength distribution, size effect on the mean fracture strength, and finally the scaling of crack surface roughness.

1. Introduction

The statistical properties of fracture in disordered media are interesting not only in view of practical applications, but also for purely theoretical reasons(1). Despite considerable progress, there exist many controversial issues between the theoretically estimated results and the experimentally measured values, and also among various theoretical and numerical models used for studying fracture of disordered media. Among these partly still controversial issues, is the scaling of crack geometries; in particular, the origin of both the scaling and the universality of the fracture surface roughness exponent is at the heart of the controversy.

From a practical applications point of view, the main issue associated with the fracture of quasi-brittle materials (such as concrete and ceramics) is the scaling of material strength; In particular, its probability distributions and its scaling with sample size, also known as the *size-effect*. In addition to understanding the universality of crack surface roughness, fracture of disordered (heterogeneous) materials poses many fundamental questions in statistical physics such as the relation between fracture and phase transitions, and the crackling noise associated with acoustic emission experiments. The importance of these acoustic emission signatures is that they are not only related to the energy release rate but also serve as a prognostic methodology

for forecasting the impending structural failure.

Experiments on several materials under different loading conditions have shown that the fracture surface is self-affine (2) and the out of plane roughness exponent displays a universal value of $\simeq 0.8$ irrespective of the material studied (3). In particular, experiments have been done in metals (4), glass (5), rocks (6) and ceramics (7), covering both ductile and brittle materials. However, the current understanding that has emerged is that crack roughness displays a universal value of $\simeq 0.8$ only at larger scales and at higher crack speeds, whereas another roughness exponent in the range of $0.4 - 0.6$ is observed at smaller length scales under quasi-static or slow crack propagation (3).

It was later shown that the roughness exponent conventionally measured describes only the local properties, while the fracture surface instead exhibits anomalous scaling (8): the *global* exponent describing the scaling of the crack width with the sample size is larger than the local exponent measured on a single sample (9; 10). It is thus necessary to define two roughness exponents a global one (ζ) and a local one (ζ_{loc}). Only the latter appears to be universal with a value $\zeta_{loc} \simeq 0.8$ (3) that is independent of the material tested (11). In comparison, the roughness exponents obtained from experiments on quasi two-dimensional materials are: $\zeta_{loc} = 0.68 \pm 0.04$ in thin wood planks (12), and $\zeta_{loc} \approx 0.73$ for crack lines in wet paper (13).

The situation that exists today is that there is a large discrepancy between theoretical estimates and experimentally measured values of roughness exponents, and hence numerical methods are in common use. A well established numerical model that deals with explicit description of disorder is based on lattice models, which describe the medium as a discrete set of elastic bonds with randomly distributed failure thresholds (1; 14; 15; 16; 17; 18). In the last 20 years, the cornerstone of fracture simulations using discrete lattice models has been the Random Fuse Model (RFM), a lattice model of the fracture of solid materials in which as a key simplification vectorial elasticity has been substituted with a scalar field. The RFM represents one of the simplest imaginable pictures of strongly interacting systems that are complicated by the presence of disorder.

The paper is organized as follows: in Section 2, we briefly describe the random fuse model. The state-of-the-art computational algorithms used for simulating fracture in the RFM are presented in Section 3. Section 4 discusses further developments in large scale simulation of fracture using high-performance computing. The scientific significance of these large scale simulations is discussed in Section 5.

2. Random Fuse Model

The RFM has been extensively investigated in the literature over the last two decades (1; 14; 15; 16; 17; 18). In the random thresholds fuse model, the lattice is initially fully intact with bonds having the same conductance, but the bond breaking thresholds, t, are randomly distributed based on a thresholds probability distribution, $p(t)$. The burning of a fuse occurs irreversibly, whenever the electrical current in the fuse exceeds the breaking threshold current value, t, of the fuse. Periodic boundary conditions are imposed in the horizontal direction to simulate an infinite system and a constant voltage difference, V, is applied between the top and the bottom of lattice system bus bars.

Numerically, a unit voltage difference, $V = 1$, is set between the bus bars and the Kirchhoff equations are solved to determine the current flowing in each of the fuses. Subsequently, for each fuse j, the ratio between the current i_j and the breaking threshold t_j is evaluated, and the bond j_c having the largest value, $\max_j \frac{i_j}{t_j}$, is irreversibly removed (burnt). The current is redistributed instantaneously after a fuse is burnt implying that the current relaxation in the lattice system is much faster than the breaking of a fuse. Each time a fuse is burnt, it is necessary to re-calculate the current redistribution in the lattice to determine the subsequent breaking of a bond. The process of breaking of a bond, one at a time, is repeated until the lattice system falls apart. In

this work, we consider a uniform probability distribution, which is constant between 0 and 1.

Numerical simulations on large system sizes are essential to understand the scaling laws of fracture and universality of crack surface roughness exponents. It is believed that roughness measurements based on numerical results obtained using large system sizes are necessary to bridge the gap that exists between numerically estimated roughness exponents and the experimentally measured roughness exponents. Unfortunately, large scale numerical simulation of these discrete lattice networks has often been hampered for two reasons.

- First, a new large set of equations has to be solved everytime a new lattice bond is broken. This becomes especially severe with increasing lattice system size, L^d (where L is the linear dimension of the lattice and d is the spatial dimension of the lattice system ($d = 2$ in 2D and $d = 3$ in 3D)), since the number of broken bonds at failure, n_f, increases with system size L as $n_f \sim \mathcal{O}(L^{1.8})$ in 2D and $n_f \sim \mathcal{O}(L^{2.7})$ in 3D.

- Second, *critical slowing down* associated with the iterative solvers close to the macroscopic fracture. That is, as the lattice system gets closer to macroscopic fracture, the condition number of the system of linear equations increases, thereby increasing the number of iterations required to attain a fixed accuracy. This becomes particularly significant for large lattices.

In addition, since the response of the lattice system corresponds to a specific realization of the random breaking thresholds, an ensemble averaging of numerical results over N_{config} configurations is necessary to obtain a realistic representation of the lattice system response. This further increases the computational time required to perform simulations on large lattice systems. In the following, we describe the state-of-the-art computational algorithms that significantly reduced the computational time thereby enabling the simulation of fracture using large lattice system sizes.

3. State-of-the-art Algorithms

Algebraically, the process of simulating fracture using discrete lattice systems is equivalent to solving a new set of linear equations

$$\mathbf{A}_n \mathbf{x}_n = \mathbf{b}_n, \qquad n = 0, 1, 2, \ldots, \tag{1}$$

every time a new lattice bond is broken. An important feature of fracture simulations using the discrete lattice systems is that, for each $n = 0, 1, 2, \ldots$, the new matrix $\mathbf{A}_{n+1}$ of the lattice system after the $(n + 1)^{th}$ broken bond is equivalent to a rank-p downdate of the matrix $\mathbf{A}_n$ (19). The matrix $\mathbf{A}_n$ refers to the lattice conductance matrix in the case of fuse models and the lattice stiffness matrix in the case of spring and beam models, $\mathbf{b}_n$ refers to the applied nodal current or force vector, and $\mathbf{x}_n$ nodal potential or displacement vector.

Traditionally, iterative techniques based on preconditioned conjugate gradient (PCG) method have been used to simulate fracture using fuse networks (see Ref. (20) for a excellent review of iterative methods; see Ref. (21) for a review of multigrid method). However, large-scale numerical simulations using iterative solvers have often been hindered due to the *critical slowing down* associated with the iterative solvers as the lattice system approaches macroscopic fracture. As a remedy, Fourier accelerated PCG iterative solvers (22; 23; 24) have been suggested to alleviate the critical slowing down. The Fourier acceleration algorithm proposed in Refs. (22; 23) chooses an ensemble averaged matrix $\bar{\mathbf{A}}$ (25; 26) as the preconditioner, where $\bar{\mathbf{A}}(i, j) = r^{(d_w - d_f)}$, $r = |i - j|$, the distance between the nodes i and j, and d_f and d_w refer to the fractal dimension of the current-carrying backbone and the random-walk dimension respectively. However, the ensemble averaged matrix $\bar{\mathbf{A}}$ is not the optimal circulant preconditioner since it does not minimize the norm $\|\mathbf{I} - \mathbf{C}^{-1}\mathbf{A}\|_F$ over all non-singular circulant matrices $\mathbf{C}$.

Even with the usage of Fourier accelerated algorithms, earlier simulations were limited to much smaller lattice systems of sizes $L = 256$ in 2D and $L = 48$ in 3D, and that too with a relatively small statistical sampling. In the following, we present two state-of-the-art algorithms, namely, the multiple sparse Cholesky downdating algorithm for 2D simulations and the block-circulant preconditioner for 3D simulations that have significantly reduced the computational time thereby enabling the simulation of fracture using much larger lattice system sizes.

3.1. Multiple-rank sparse Cholesky downdating algorithm

An important feature of fracture simulations using discrete lattice models is that, for each $n = 0, 1, 2, \ldots$, the new matrix $\mathbf{A}_{n+1}$ of the lattice system after the $(n + 1)^{th}$ broken bond is equivalent to a rank-p downdate of the matrix $\mathbf{A}_n$ (19; 27). Mathematically, in the case of the fuse and spring models, the breaking of a bond is equivalent to a rank-one downdate of the matrix $\mathbf{A}_n$, whereas in the case of beam models, it is equivalent to multiple-rank (rank-3 for 2D, and rank-6 for 3D) downdate of the matrix $\mathbf{A}_n$. Thus, an updating scheme of some kind is therefore likely to be more efficient than solving the new set of equations formed by Eq. (1) for each n.

Consider the Cholesky factorizations

$$\mathbf{P}\mathbf{A}_n\mathbf{P}^t = \mathbf{L}_n\mathbf{L}_n^t \tag{2}$$

for each $n = 0, 1, 2, \cdots$, where $\mathbf{P}$ is a permutation matrix chosen to preserve the sparsity of $\mathbf{L}_n$. Since the breaking of bonds is equivalent to removing the edges in the underlying graph structure of the matrix $\mathbf{A}_n$, for each n, the sparsity pattern of the Cholesky factorization $\mathbf{L}_{n+1}$ of the matrix $\mathbf{A}_{n+1}$ must be a subset of the sparsity pattern of the Cholesky factorization $\mathbf{L}_n$ of the matrix $\mathbf{A}_n$. Hence, for all n, the sparsity pattern of $\mathbf{L}_n$ is contained in that of $\mathbf{L}_0$. That is, denoting the sparsity pattern of $\mathbf{L}$ by $\mathcal{L}$, we have

$$\mathcal{L}_m \supseteq \mathcal{L}_n \quad \forall\, m < n \tag{3}$$

For two-dimensional lattice simulations, in Ref. (19), we proposed an efficient algorithm based on multiple-rank sparse Cholesky downdating scheme of Davis and Hager (28; 29) to successively downdate the Cholesky factorizations $\mathbf{L}_n$ of $\mathbf{A}_n$ to $\mathbf{L}_{n+1}$ of $\mathbf{A}_{n+1}$, i.e., $\mathbf{L}_n \rightarrow \mathbf{L}_{n+1}$ for $n = 0, 1, 2, \cdots$. Since $\mathcal{L}_n \supseteq \mathcal{L}_{n+1}$, it is necessary to modify only a part of the non-zero entries of $\mathbf{L}_n$ in order to obtain $\mathbf{L}_n \rightarrow \mathbf{L}_{n+1}$. This results in a significant reduction in the computational time. Once the factorization $\mathbf{L}_{n+1}$ of $\mathbf{A}_{n+1}$ is obtained, the solution vector $\mathbf{x}_{n+1}$ is obtained from $\mathbf{L}_{n+1}\mathbf{L}_{n+1}^t\mathbf{x}_{n+1} = \mathbf{b}_{n+1}$ by two triangular solves (19). Using this algorithm (19), the authors have reported numerical simulation results for large 2D lattice systems (e.g., $L = 1024$), which to the authors knowledge, was so far the largest lattice system used in studying damage evolution using discrete lattice systems.

3.2. Optimal and superoptimal circulant preconditioners

Although the sparse direct solver algorithm presented in (19) is superior to iterative solvers in two-dimensional lattice systems, for 3D lattice systems, the memory demands brought about by the amount of *fill-in* during sparse *Cholesky* factorization favor iterative solvers. The main observation behind developing preconditioners for the iterative schemes is that the operators on discrete lattice network result in a circulant block structure. Hence, a fast Poisson type solver with a circulant preconditioner can be used to obtain the solution in $\mathcal{O}(N\, logN)$ operations using FFTs of size N, where N denotes the number of degrees of freedom. However, as the lattice bonds are broken successively, the initial uniform lattice grid becomes a diluted network. Consequently, although the matrix $\mathbf{A}_0$ is Toeplitz (also block Toeplitz with Toeplitz blocks) initially, the subsequent matrices $\mathbf{A}_n$, for each n, are not Toeplitz matrices. However, depending

on the pattern of broken bonds, $\mathbf{A}_n$ may still possess block structure with many of the blocks being Toeplitz blocks.

The authors have developed an algorithm based on a block-circulant preconditioned conjugate gradient (CG) iterative scheme (30) for simulating 3D random fuse networks. The block-circulant preconditioner was shown to be superior compared with the *optimal* point-circulant preconditioner for simulating 3D random fuse networks (30). Since these block-circulant and *optimal* point-circulant preconditioners achieve favorable clustering of eigenvalues, these algorithms significantly reduced the computational time required for solving large lattice systems in comparison with the Fourier accelerated iterative schemes used for modeling lattice breakdown (24; 31).

Using this block circulant preconditioner, we were able to simulate fracture in lattice systems of sizes up to $64 \times 64 \times 64$, which is the largest ever discrete lattice system used in 3D for fracture simulation of broadly disordered materials. The simulation begins with an intact lattice system and is carried out by breaking one bond at a time until the macroscopic fracture occurs. Table 1 presents a summary of computational times required for simulating the fracture of one such sample configuration of a 3D cubic lattice system. These simulations have been performed on a IBM 1.3 GHz Power4 processor. The CPU times taken for simulating a cubic lattice system of size $(L \times L \times L)$ scales as $\mathcal{O}(L^{6.5})$, which poses severe computational requirements for simulating fracture of even larger lattice system sizes that are required to obtain accurate scaling laws of fracture in 3D. This is precisely the scenario where massively parallel simulation offers significant advantages. In the following, we present massively parallel simulations of large 3D lattice systems for studying fracture of disordered materials.

Table 1: Block Circulant PCG (3D Cubic Lattice)

Size	CPU(sec)	Iterations
10	16.54	16168
16	304.6	58756
24	2154	180204
32	12716	403459
48	130522	1253331
64	1180230	

4. High-Performance Computing

Since iterative solvers exhibit excellent scalability with respect to number of processors, parallel iterative solvers are especially suitable for performing large scale fracture simulations using 3D lattice networks. Using PETSc (32; 33; 34), we were able to start from our existing serial code and rapidly parallelize the most time-consuming (solvers) portions of the computation. At each simulation step, the PETSc `KSPSolve()` routine is used to solve for the current flowing in each of the fuses using a parallel preconditioned Krylov iterative solver; in the simulations described here, we used conjugate gradient with a block-Jacobi preconditioner in which ILU(0) was applied on each block. The preconditioner we chose is likely not ideal for this system, but has the advantage of being highly parallel. Because the coefficient matrices between steps differ only by a rank-1 update, we do not update the ILU(0) factors at each step; in our simulations we recalculated the factors every 1000 steps.

Using PETSc, fracture of a $L = 64$ cubic lattice system can be simulated within 3 hours (compare this with 14 days of CPU time on a single processor using the block-circulant preconditioner) on 128 Cray-XT3 processors (2.4 GHz). Our largest simulation, a fracture simulation on a lattice system of size $L = 100$ in 3D requires a day of computational time on

512 processors of Cray-XT3 (see Fig. 1 for comparison of performance scaling on Cray-XT3 and Blue-Gene/L at Argonne). Figure 1 illustrates the performance of our parallel code on a 100^3 lattice benchmark for up to 1024 processors. Performance on both the BlueGene/L and Cray XT3 systems is encouraging, especially given the rapidly-prototyped nature of our code. Currently, we are simulating fracture of 3D lattice systems of sizes up to $L = 200$, which is significant not only because of this first ever computational achievement but also because of the scientific results such as scaling laws and size effects that are obtained from these largest ever system size simulations.
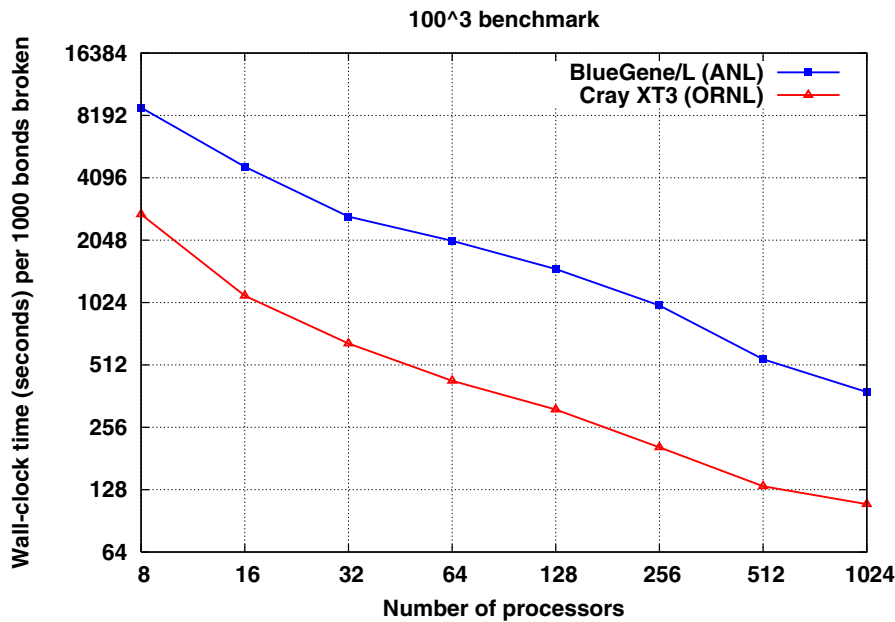
Figure 1. Performance comparison of the parallel RFM code in simulating a large 3D cubic lattice system of size $L = 100$ on Cray-XT3 (Jaguar) at ORNL and on Blue-Gene/L at ANL.

Along with massive parallelization, it may be worthwhile to look into alternative algorithmic strategies/preconditioners for solving the system of equations that arise in the simulation of large 3D lattice systems. Currently, we are pursuing recycling of Krylov subspaces (35) determined while solving $\mathbf{A}_n \mathbf{x}_n = \mathbf{b}_n$ and use it to reduce the cost of solving the subsequent system $\mathbf{A}_{n+1} \mathbf{x}_{n+1} = \mathbf{b}_{n+1}$ with minimal effort. Such a recycling process amounts to a reduction of iteration count required to solve the new linear system $\mathbf{A}_{n+1} \mathbf{x}_{n+1} = \mathbf{b}_{n+1}$, and hence increases the overall efficiency of the algorithm. Our preliminary work using these recycled subspaces resulted in an algorithm that is 30% faster than the corresponding algorithm that does not use recycling techniques.

5. Scientific Significance

In the following, we present the significant scientific results that are obtained through these large scale simulations. We focus on four different aspects of fracture in disordered systems. First of all, we resolve the long standing controversy whether damage and (even possibly correlated) percolation are in the same universality class. Second, our numerical results resolve the issue of whether fracture is akin to a first-order or second-order phase transition. Third, we show that for strongly disordered systems, a lognormal distribution is a better fit for fracture strength distribution than the classical Weibull or Gumbel distributions. In addition, we resolve the

inconsistency between the logarithmic size effect observed in statistical physics models and the more traditional inverse square root size effect observed in classical engineering fracture models. Lastly, our numerical results show for the first time that crack surface roughness exhibits anomalous scaling as observed in recent experiments on granite and wood samples. In addition, we note that multiscaling of crack surface roughness is observed only at small scales and crosses over to a self-affine scaling at large scales.

5.1. Damage and Percolation

Disorder and long-range interactions are two of the key components of material failure. When the disorder is narrowly (weakly) distributed, materials breakdown without significant precursors. As the disorder increases, substantial damage is accumulated prior to failure and the dynamics resembles percolation. Indeed, in the limit of infinite disorder, the damage accumulation process can exactly be mapped onto a percolation problem. An interesting question is whether damage accumulation in the case of broad (large, but finite) disorder is in the same universality class as percolation.

Using simulations on small system sizes, Hansen and Schmittbuhl (36) have argued that fracture of broadly disordered systems is in the same universality as that of uncorrelated percolation. Based on the similarities with percolation, they (36) suggested the following finite size scaling law for the fraction of broken bonds, given by

$$p_f - p_c \quad \sim \quad L^{-\frac{1}{\nu}} \sim N_{el}^{-\frac{1}{d\nu}} \tag{4}$$

In the Eq. (4), p_f and p_c represent the fracture thresholds in a lattice system size of L and infinity, respectively, and d denotes the dimension ($d = 2$ in 2D and $d = 3$ in 3D). As the system size $L \to \infty$, the broken bonds at failure $p_f \to p_c$. The correlation critical exponent ν was found in Ref. (36) to be consistent with the percolation value $\nu = 4/3$. An additional test is provided by the damage standard deviation at failure Δ_f (31) which should scale as

$$\Delta_f \quad \sim \quad L^{-\frac{1}{\nu}} \sim N_{el}^{-\frac{1}{d\nu}} \tag{5}$$

Using our large scale simulations that span a wider finite size range than that of Ref. (36), wherein simulations with sizes up to $L = 60$ are used, we tested this percolation hypothesis and found that the the mean fraction of broken bonds at failure p_f does not scale linearly with $N_{el}^{-3/8}$ for system sizes $L > 100$. While to accept the percolation hypothesis one should observe a linear regime, a net curvature is apparent in the data especially for sizes $L > 100$. The same result is obtained with a very broad disorder or thresholds distribution (37). Using these large scale simulations, we have also resolved the controversy that fracture is akin to a correlated percolation (see Ref. (37)).

5.2. First-order or Second-order Phase Transition

A long standing controversy in statistical physics of fracture is whether fracture is akin to a first-order or second-order phase transion. The data from our large scale simulations and extensive statistical sampling for various lattice system sizes and various lattice topologies indicate that the cumulative probability distribution for the fraction of broken bonds at failure (also termed as cumulative failure probability distribution) can be collapsed onto a single master curve suggesting that the failure probability distribution is universal. In addition, our data suggest that a Gaussian distribution adequately describes the failure probability distribution (37).

The fact that damage is Gaussian distributed suggests that there is no divergent correlation length at failure. Long-range correlations in the damage would imply that the central limit theorem does not hold and hence the normal distribution would not be an adequate fit to the
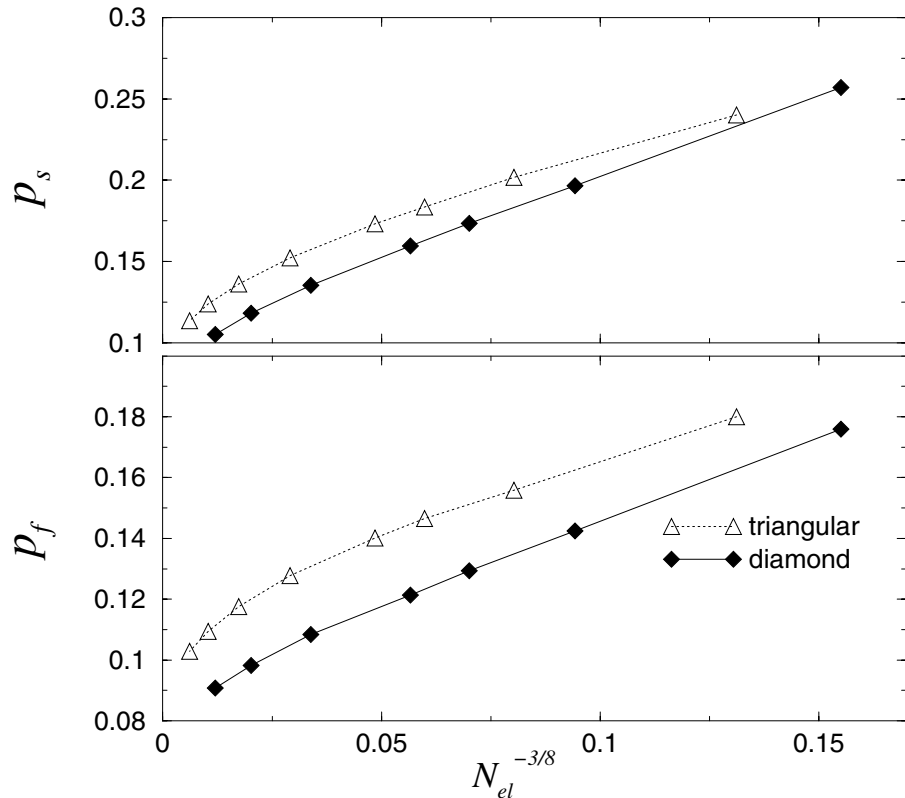
Figure 2. The 50% survival probability p_s (top) and the mean fraction of broken bonds p_f (bottom) plotted as a function of $N_{el}^{-3/8}$ for the uniform threshold distribution. If percolation scaling is obeyed, the data should follow a straight line. A net curvature is instead observed in all the data for large lattice sizes.

data. The absence of long-range corralation is again in agreement with the hypothesis that fracture is analogous to a first-order transition (16; 37).

5.3. Fracture Strength and Size Effects

Traditionally, Weibull and (modified) Gumbel distributions based on "weakest-link" approach have been widely used to describe the strength of brittle materials. These distributions naturally arise from extreme-value statistics of defect cluster distributions. However, in heterogeneous materials with broad distribution of disorder, Weibull and Gumbel distributions may not adequately represent the fracture strengths corresponding to the peak load response (38).

The results of our large scale simulations allow to determine the form of the fracture strength distribution and its dependence on the lattice size. Figure 3 shows the fracture strength density distributions for random thresholds fuse and spring models using the standard Lognormal variable, $\bar{\xi}$, defined as $\bar{\xi} = \frac{Ln(\sigma_f) - \eta}{\zeta}$, where σ_f refers to the fracture strength defined as the peak load divided by the system size L, and η and ζ refer to the mean and the standard deviation of the logarithm of σ_f. The excellent collapse of the data for various fuse and spring lattices clearly indicates the universality of the fracture strength density distribution.

In addition, the collapse of the data in Fig. 3 suggests that $P(\sigma \leq \sigma_f) = \Psi(\bar{\xi})$, where $P(\sigma \leq \sigma_f)$ refers to the cumulative probability of fracture strength $\sigma \leq \sigma_f$, Ψ is a universal function such that $0 \leq \Psi \leq 1$, and $\bar{\xi} = \frac{Ln(\sigma_f) - \eta}{\zeta}$ is the standard Lognormal variable. The

inset of Fig. 3 presents a Lognormal fit for fracture strengths, tested by plotting the inverse of the cumulative probability, $\Phi^{-1}(P(\sigma_f))$, against the standard Lognormal variable, $\bar{\xi}$. In the above description, $\Phi(\cdot)$ denotes the standard normal probability function. As discussed in Ref. (39), a Lognormal distribution is an adequate fit for 3D random fuse models as well. This further confirms the notion of universality of fracture strength distribution in broadly disordered materials.
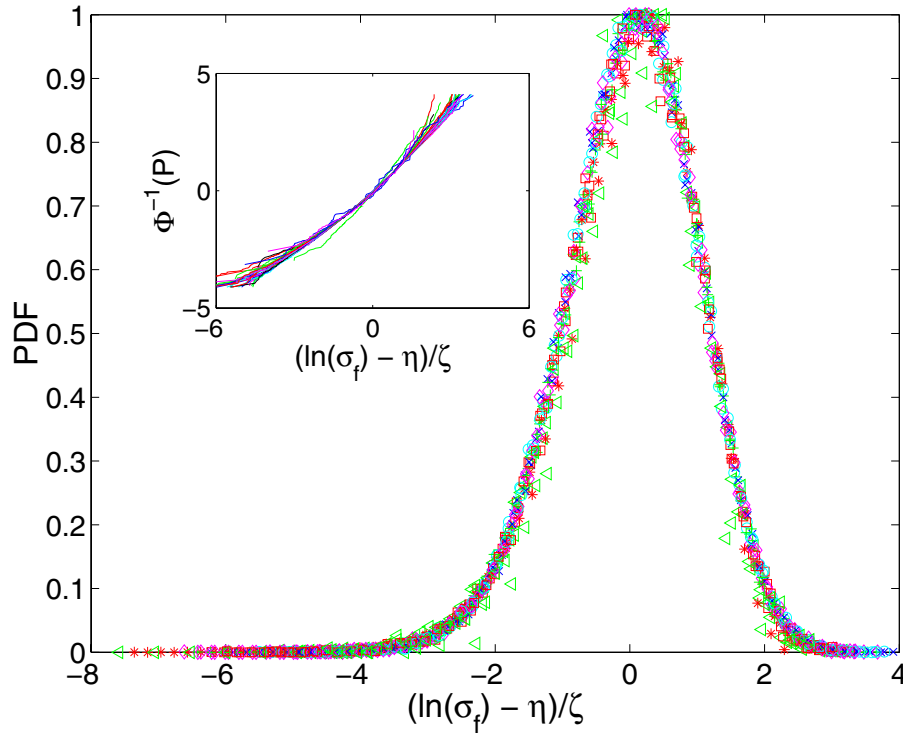
Figure 3. Universality of fracture strength distribution in the random thresholds fuse and spring models. Data are for different lattice system sizes, L, corresponding to triangular fuse lattice with uniform disorder ($L = \{4, 8, 16, 24, 32, 64, 128\}$), diamond fuse lattice with uniform disorder ($L = \{4, 8, 16, 24, 32, 64, 128\}$), triangular fuse lattice with power law disorder ($L = \{4, 8, 16, 24, 32, 64, 128\}$), and triangular spring lattice with uniform disorder ($L = \{8, 16, 24, 32, 64, 128\}$). The inset reports a Lognormal fit for the corresponding cumulative distributions.

5.3.1. Strength of Notched Specimens   The statistical physics models predict a logarithmic size effect in the unnotched specimens. However, from an engineering point of view, scaling of fracture strength in pre-notched specimens is of significant interest (40; 41; 42; 43; 44). The size effect in this case is often given by a scaling of the form $\mu_f \propto a^{-1/2}$, where $a = a_0 + c_f$ is the effective crack size, a_0 is the initial crack (notch) size, and c_f is the FPZ size surrounding the crack tips (40; 41; 42; 43; 44). This study bridges the gap between $a^{-1/2}$ size effect in the engineering literature (40; 41; 42; 43; 44) and the typical logarithmic size effect in the statistical physics literature, and this difference is due to two aspects: i) initial relative crack size a_0/L, and ii) disorder.

The size effects obtained in such notched specimens using the 2D RFM with uniform thresholds disorder are presented in Fig. 4. The data shows the scaling of fracture strength

with system size for a fixed initial crack size, a_0/L. The results can be fitted by a power law of the type

$$\mu_f \propto L^{-m}, \tag{6}$$

where the scaling exponent m is significantly influenced by a_0/L: for small a_0/L values, m is very small, and is equivalent to a logarithmic correction as in unnotched specimens while for large a_0/L values, m approaches $1/2$ as predicted by LEFM (40). The reason for this behavior is that in the small a_0/L regime, fracture is dominated by disorder, whereas in the large a_0/L regime, fracture is controlled by the initial crack. Similarly, a weak disorder leads to the standard $m = 1/2$ scaling, while for strong disorder we have a logarithmic size effect.
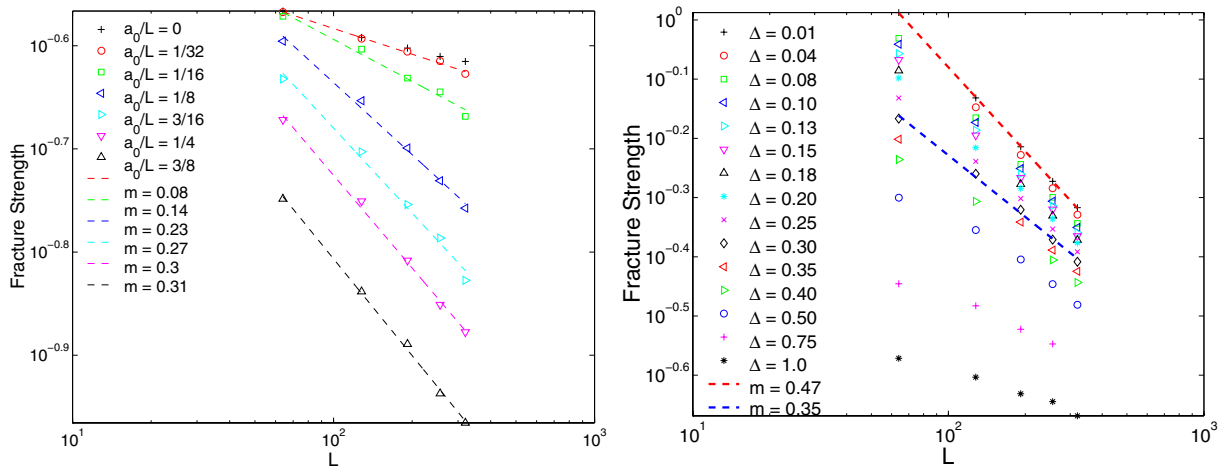
Figure 4. Size effects in notched specimens with uniform thresholds disorder. The effective scaling exponent of mean fracture strength depends on (a) the ratio a_0/L. (b) the disorder Δ.

5.4. Crack Roughness

Lattice models for fracture have been used in the past to analyze the roughness of the crack surfaces in various geometries. The RFM has been numerically simulated in two (11; 45; 46; 47) and three dimensions (24; 47) using various types of disorder. Due to numerical limitations, earlier numerical simulations mostly considered global measurements for the crack roughness, while more recent results explored other quantities and the possibility of anomalous scaling.

In Fig. 5a we report the local width for triangular random fuse lattices for different sizes L. The curves for different system sizes do not overlap even for $l \ll L$ which would be the scenario when anomalous scaling is present. The global width scales with an exponent $\zeta = 0.83 \pm 0.02$ (11). On the other hand the local width increases with a smaller exponent, that can be estimated for the larger system sizes as $\zeta_{loc} \simeq 0.7$. The data reported in Fig. 5b are collapsed using $\zeta - \zeta_{loc} = 0.13$. More precise values for the local and global roughness exponents are obtained from the power spectrum results, which yields instead a local exponent $\zeta_{loc} = 0.74$, implying $\zeta = 0.87$ for the global exponent. Although the value of $\zeta - \zeta_{loc}$ is small, it is significantly larger than zero so that we would conclude that anomalous scaling is present.

Our recently performed extensive simulations of 3D RFM have obtained similar results. In particular, an analysis of the width and the power spectrum data results in a value of $\zeta \simeq 0.52$, with possible anomalous scaling corresponding to a local value of $\zeta_{loc} \simeq 0.42$ (see Fig. 6). Finally, our results on notched specimens indicate that the roughness is neither dependent on the disorder nor on the a_0/L ratio.
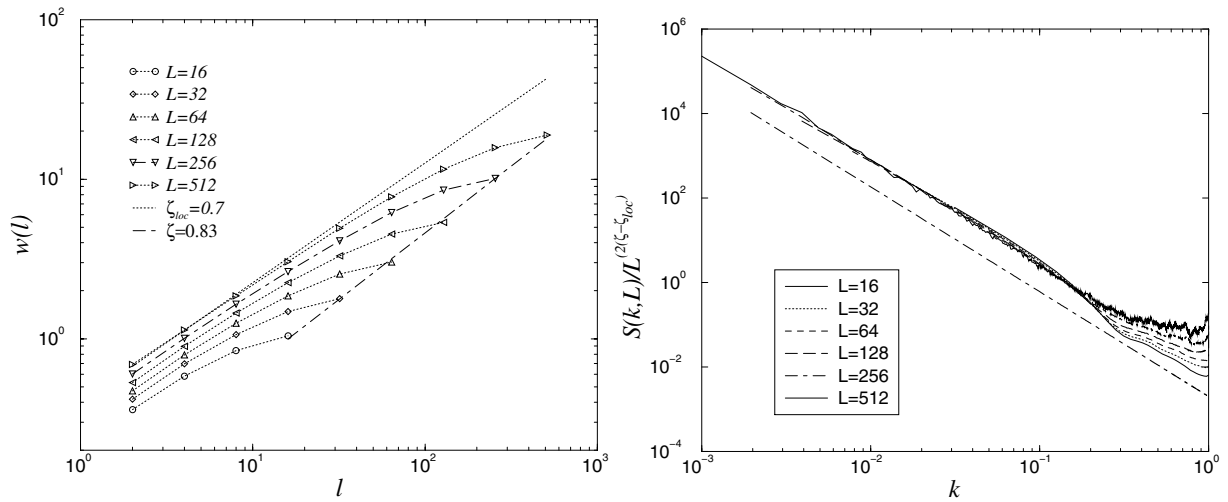
Figure 5. (a) The local width $w(l)$ of the crack surface for different lattice sizes of 2D RFM triangular lattice systems plotted in log-log scale. A line with the local exponent $\zeta_{loc} = 0.7$ is plotted for reference. The global width displays an exponent $\zeta > \zeta_{loc}$.(b) The corresponding power spectrum in log-log scale. The spectra for all of the different lattice sizes can be collapsed indicating anomalous scaling.
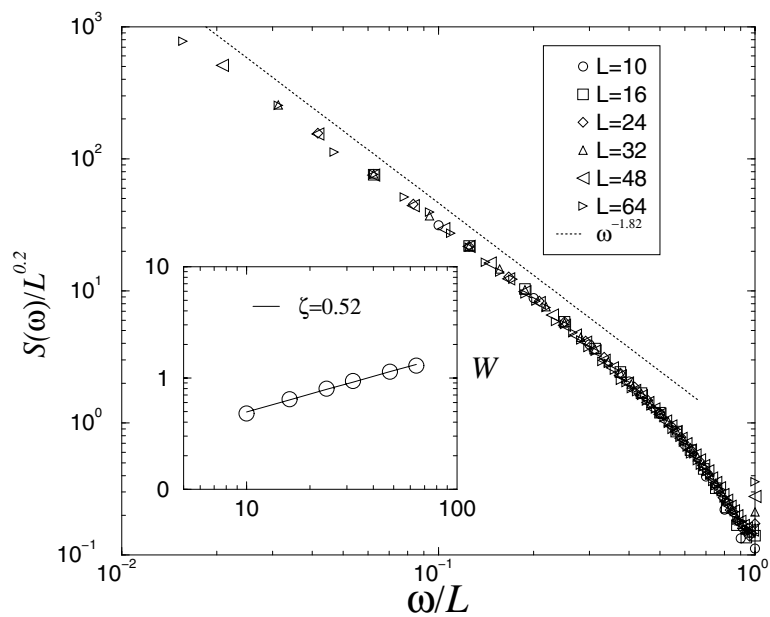

Figure 6. The power spectrum of the crack surface of the three dimensional RFM. The spectrum exponent $2\zeta + 1 = 1.82$, corresponds to $\zeta_{loc} = 0.41$. The global width scales with $\zeta = 0.52$ (see inset), so that the power spectrum should be normalized by $2(\zeta - \zeta_{loc}) \simeq 0.2$

6. Conclusions

We have presented two state-of-the-art algorithms for simulating fracture of disordered quasi-brittle materials using 2D and 3D discrete lattice systems. These algorithms have enabled us to simulate fracture of largest ever lattice systems, which are necessary to obtain accurate scaling laws of fracture. We have further expanded this finite size scaling regime using massively parallel simulations on thousands of processors of Cray-XT3 (Jaguar) and IBM Blue-Gene/L. Using these parallel algorithms, we can currently simulate fracture of a 3D lattice system of size $L = 64$ within 3 hours on Cray-XT3 (within 9 hours on IBM Blue-Gene/L), whereas it requires 14 days of computational time on a single processor. We can currently simulate fracture of 3D lattice systems of sizes up to $L = 200$, which is a significant computational achievement considering that traditionally fracture of lattice systems of sizes up to $L = 48$ were simulated, and that computational complexity increases as $\mathcal{O}(L^{6.5})$.

The numerical results obtained through these large scale system sizes in conjunction with extensive statistical sampling have advanced the current understanding of physics of fracture. In particular, these large scale simulations have been instrumental in understanding the following aspects of fracture phenomena:

- Fracture of strongly disordered systems is not in the same universality class as that of (uncorrelated or even possibly correlated or gradient) percolation. Damage is accumulated in an uniform manner in the pre-peak regime and then suddenly localizes in the post-peak regime. Damage profiles are unform in the pre-peak regime, and show a peak with exponential tails in the post-peak regime.

- The failure probability distribution (both in 2D and 3D) is universal and is Gaussian, which indicates a lack of divergent correlation length thereby suggesting that fracture is akin to a first-order phase transition.

- For broadly disordered material systems, fracture strength distribution follows neither the classical Weibull nor the Gumbel distributions. Instead, a lognormal distribution appears to represent the fracture strength distribution adequately. For unnotched samples, we obtain a logarithmic size effect on the mean fracture strength. However, the size-effect depends crucially on the relative crack size a_0/L in the notched samples, and on the amount of disorder. We show for the first time that as the relative crack size or the disorder is varied, the size-effect transitions from a logarithmic size effect to the $1/\sqrt{(a_0)}$ observed in classical LEFM.

- Our large scale numerical results show for the first time that crack surface roughness exhibits anomalous scaling as observed in recent experiments on granite and wood samples. This was not possible in earlier simulations due to small system sizes. The local roughness is estimated to be 0.72 ± 0.03 and is universal, whereas the global roughness is estimated to be 0.83 ± 0.04. In addition, the global width distribution is found to be universal as well.

References

[1] Herrmann H J and Roux S (eds.) 1990 *Statistical Models for the Fracture of Disordered Media*, (North-Holland, Amsterdam). Chakrabarti B K and Benguigui L G 1997 *Statistical physics of fracture and breakdown in disordered systems* (Oxford Univ. Press, Oxford)

[2] Mandelbrot B B, Passoja D E and Paullay A J 1984 *Nature* (London) **308**, 721

[3] For a review see Bouchaud E 1997 *J Phys. C* **9**, 4319

[4] Maloy K J, Hansen A, Hinrichsen E L and Roux S 1992 *Phys. Rev. Lett.* **68**, 213; Bouchaud E, Lapasset G, Planés J and Navéos S 1993 *Phys. Rev. B* **48**, 2917

[5] Daguier P, Nghiem B, Bouchaud E and Creuzet F 1997 *Phys. Rev. Lett.* **78**, 1062

[6] Schmittbuhl J, Roux S and Berthaud Y 1994 *Europhys. Lett.* **28**, 585 Schmittbuhl J, Schmitt F and Scholz C 1995 *J. Geophys. Res.* **100**, 5953

[7] Mecholsky J J, Passoja D E and Feinberg-Ringel K S 1989 *J. Am. Ceram. Soc.* **72**, 60

[8] López J M, Rodríguez M A and Cuerno R 1997 *Phys. Rev. E* **56**, 3993

[9] López J M and Schmittbuhl J 1998 *Phys. Rev. E* **57**, 6405

[10] Morel S, Schmittbuhl J, López J M and Valentin G 1998 *Phys. Rev. E* **58**, 6999

[11] Nukala P K V V, Zapperi S and S. Simunovic S 2005 *Phys. Rev. E* **71**, 066106

[12] Engoy T, Maloy K J, Hansen A and Roux S 1994 *Phys. Rev. Lett.* **73**, 834

[13] Kertész J, Horváth V K and Weber F 1993 *Fractals* **1**, 67; Rosti J, Salminen L I, Seppälä E T, Alava M J and Niskanen K J 2001 *Eur. Phys. J.* B **19**, 259; Salminen L I, Alava M J and Niskanen K J 2003 *ibid* **32**, 369

[14] de Arcangelis L, Redner S and Herrmann H J 1985 *J. Phys. (Paris) Lett.* **46** 585

[15] Sahimi M and Goddard J D 1986 *Phys. Rev. B* **33**, 7848

[16] Zapperi S, Ray P, Stanley H E and Vespignani A 1997 *Phys. Rev. Lett.* **78**, 1408; 1999 *Phys. Rev. E* **59**, 5049

[17] Hansen A and Roux S 2000 *Statistical toolbox for damage and fracture*, 17-101, in book *Damage and Fracture of Disordered Materials*, eds. Krajcinovic D and van Mier J G M, Springer Verlag, New York.

[18] Alava M J, Nukala P K V V and Zapperi S 2006 *Advances in Physics* (in press)

[19] Nukala P K V V and Simunovic S 2003 *J. Phys. A: Math. Gen.* **36**, 11403

[20] Barrett R et. al. 1994 *Templates for the Solution of Linear Systems: Building Blocks for Iterative Methods, 2nd Edition*, SIAM, Philadelphia

[21] Briggs W L, Van Emden Henson and McCormick S F 2000 *A Multigrid Tutorial, 2nd Edition*, SIAM, Philadelphia

[22] Batrouni G G, Hansen A and Nelkin M 1986 *Phys. Rev. Lett.* **57**, 1336

[23] Batrouni G G, Hansen A and Nelkin M 1988 *J. Stat. Phys.* **52**, 747

[24] Batrouni G G and Hansen A 1998 *Phys. Rev. Lett.* **80**, 325

[25] O'Shaughnessy and Procaccia I 1985 *Phys. Rev. Lett.* **54**, 455

[26] O'Shaughnessy and Procaccia I 1985 *Phys. Rev. A* **32**, 3073

[27] Nukala P K V V, Simunovic S and Guddati M N 2005 *Int. J. Numer. Meth. Engng.* **62**, 1982

[28] Davis T A and Hager W W 1999 *SIAM J. Matrix Anal. Appl.* **20**(3), 606-27

[29] Davis T A and Hager W W 2001 *SIAM J. Matrix Anal. Appl.* **22**(4), 997-1013

[30] Nukala P K V V, and Simunovic S 2004 *J. Phys. A: Math. Gen.* **37**, 2093

[31] Ramstad T, Bakke J O H, Bjelland J, Stranden T and Hansen A 2004 *Phys. Rev.* E **70**, 036123

[32] Balay S et. al. 2001 *http://www.mcs.anl.gov/petsc*

[33] Balay S et. al. 2004 *ANL-95/11 - Revision 2.1.5*, Argonne National Laboratory, Argonne, IL

[34] Balay S et. al. 1997 *Modern Software Tools in Scientific Computing*, 163-202, (Birkhäuser Press).

[35] Parks M L, de Sturler E, Mackey G, Johnson D D and Maiti S 2006 *SIAM Journal on Scientific Computing* (in press)

[36] Hansen A and Schmittbuhl J 2003 *Phys. Rev. Lett.* **90**, 45504

[37] Nukala P K V V, Simunovic S and Zapperi S 2004 *J. Stat. Mech.: Theor. Exp.* P08001

[38] Nukala P K V V and Simunovic S 2004 *Eur. Phys. J.* B **37**, 91

[39] Zapperi S and Nukala P K V V 2006 *Int. J. Fracture* (in press)

[40] Bazant Z P 1999 *Arch. Appl. Mech.* **69**, 703

[41] Bazant Z P et. al. 2002 *Int. J. Fracture* **113**, 345

[42] Bazant Z P 2004 *Probabilistic Engineering Mechanics* **19**, 307

[43] Bazant Z P 2004 *PNAS* **101**, 13400

[44] Bazant Z P and Yavari A 2005 *Engineering Fracture Mechanics* **72**, 1

[45] Hansen A, Hinrichsen E L and Roux S 1991 *Phys. Rev. Lett.* **66**, 2476

[46] Räisänen V I, Seppala E T, Alava M J and Duxbury P M 1998 *Phys. Rev. Lett.* **80**, 329

[47] Räisänen V I, Alava M J and Nieminen R M 1998 *Phys. Rev.* B **58**, 14288